



Contents lists available at ScienceDirect

Materials Today: Proceedings

journal homepage: www.elsevier.com/locate/matpr

Numerical simulation and optimization of p-NiO/n-TiO₂ solar cell system using SCAPS

R.T. Mouchou^{a,*}, T.C. Jen^{a,**}, O.T. Laseinde^a, K.O. Ukoba^a

^a University of Johannesburg, Johannesburg, Kingsway and University Road, Auckland Park, Johannesburg 2006, South Africa

ARTICLE INFO

Article history:

Received 9 March 2020

Received in revised form 26 April 2020

Accepted 29 April 2020

Available online 19 June 2020

Keywords:

Nanostructure

Science

Numerical simulation

Solar cell

SCAPS

Material

ABSTRACT

This study illustrates a numerical simulation and optimization of NiO/TiO₂ metal oxide thin film for solar cell applications. Metal oxide-based solar cells have now become a new and low-cost alternative for sunlight harvesting and solar power generation. Different material properties like thickness, temperature, and density of states for conduction and valence band were varied using the SCAPS 1D template. The study examined various window layer material with varied range of 300 K –400 K temperature. Therefore, the thickness are also varied between 2 to 0.05 μm and the interface state 1018 to 1021 for absorber and buffer respectively. The objective of this study is to show the numerical annealing effect on the efficiency of nanostructured p-NiO/n-TiO₂ heterojunction solar cells using Solar Cells Capacitance Simulator (SCAPS). As the p-NiO layer reduced at high thickness the electrons and holes have more time to recombine whereby the increase in thickness also presented more than 100% increase in fill factor (FF) with the efficiency that was varied from 0.03 to 0.05. The analyzed result indicates that the thickness increase in J_{sc}, FF, density, and efficiency is due to more electron holes pairs generated.

© 2020 Elsevier Ltd. All rights reserved.

Selection and peer-review under responsibility of the scientific committee of the International Symposium on Nanostructured, Nanoengineered and Advanced Materials. This is an open access article under the CC BY-NC-ND license (<http://creativecommons.org/licenses/by-nc-nd/4.0/>).

1. Introduction

Energy is a crucial feature for social-economic growth and development. The goal of energy transformation is to provide access to energy to improve the quality of life and enhance productivity [1]. Currently, electrical energy is widely generated using fossil fuels [2]. However, the continued use of fossil fuels is not environmentally friendly because of the greenhouse gas emission associated with the use of fossil fuels [1]. Access to electricity has a direct link to good health, agriculture activities and plays a major role in the realization of sustainable development goals [2]. As such, countries must consider measures that will ensure uninterrupted power supply.

Several countries still struggle to deliver affordable, efficient and stable electricity [3]. Present statistics reveals that 87% of the 1.5 billion population of people living in Africa are among the world's highest number within developing countries, without access to electricity [4]. This implies that there is an energy deficit

that needs to be met to ensure that more people have access to electricity [5]. The energy deficit should also be met without generating electricity through sources that pose a threat to the environment. The use of renewable energy technologies such as solar energy is suitable to meet this demand. Renewable energy such as solar cells has been recognized to be a viable solution to satisfy the energy deficit and also reduce the environmental problems arising from the use of fossil fuels [6]. In several countries, there is a vast amount of sunlight to support electricity generation from solar cells [7]. Solar radiation can be converted to direct current electricity via solar cells [8].

The appeal of solar cells for the generation of electricity from incident solar radiation has necessitated the conduct of research in different areas [9]. An important area in this regard is the design of solar cells with enhanced physical properties [10]. The physical properties of the solar cell influence their energy generation efficiency. Examples of physical properties of solar cells are density, temperature, and thickness. Simulation has been used for the optimization of the parameters that influence the generation of electricity from solar energy [1].

* Primary corresponding author.

** Second corresponding author.

<https://doi.org/10.1016/j.matpr.2020.04.880>

2214-7853/© 2020 Elsevier Ltd. All rights reserved.

Selection and peer-review under responsibility of the scientific committee of the International Symposium on Nanostructured, Nanoengineered and Advanced Materials. This is an open access article under the CC BY-NC-ND license (<http://creativecommons.org/licenses/by-nc-nd/4.0/>).

Please cite this article as: R. T. Mouchou, T. C. Jen, O. T. Laseinde et al., Numerical simulation and optimization of p-NiO/n-TiO₂ solar cell system using SCAPS, Materials Today: Proceedings, <https://doi.org/10.1016/j.matpr.2020.04.880>

The design of potential photovoltaic (PV) materials aims to address the issues of realizing high energy efficiency, low cost, and stability [9]. The realization of these performance goals should be considered during the doping of semiconductors used in designing solar cells. Suitable semiconductors for designing solar cells with high performance can be realized from the non-conventional doping of layered p-n type material. All the potential alternative photovoltaic (PV) materials, introduced recently, need to address three major issues: high efficiency, low cost, and stability [11]. Non-conventional doping layered type material under transition metal [12]. It has been under extensive research for the last few years due to the great potentiality of fabricating highly efficient solar cells [13].

The paper presents simulation results of NiO/TiO₂ p-n heterojunction solar cells owing to the numerous uncertainty such as defect, thermal or electrical properties mismatches associated with experiment [14]. This is intending to provide a useful guideline for the experimental design of high-performance metal oxide-based solar cells.

2. Numerical simulation

This numerical analysis employed SCAPS (Solar Cell Capacitance Simulator) a software version 3.3.00 originally designed for polycrystalline thin-films, CdTe and CIGS solar cells. The AC and DC electrical measurements which can be simulated on SCAPS include open-circuit voltage (V_{oc}), short circuit current density (J_{sc}), fill factor (FF%), quantum efficiency (QE%), efficiency percentage, generation and recombination profiles, heterojunction energy band structure, etc. All these measurements can be calculated and obtained in dark and light conditions at different temperatures and illuminations. Up to seven layers can be added to the cell structure in SCAPS problem setting window while the physical and electronic properties of these layers and contacts should be imported into their specific sections.

SCAPS solves the basic semiconductor equations namely the Poisson's equations for electrons and holes (1); the equations of continuity for electrons and holes (2) and the carrier transport equations for electrons and holes (3) to obtain the J-V performance of each simulated solar cell architectures [15].

$$\frac{d^2\varphi(x)}{dx^2} = \frac{e}{\varepsilon_0\varepsilon_r} (p(x) - n(x) + N_D - N_A + \rho_p - \rho_n) \quad (1)$$

where φ , e , ε_0 , ε_r , N_D , N_A , ρ_p and ρ_n are the electrostatic potential, electrical charge, vacuum permittivity, relative permittivity, charged impurities of donor, charged impurities of acceptor, holes distribution and electrons distribution.

$$\frac{dJ_n}{dx} = G - R \quad (2a)$$

$$\frac{dJ_p}{dx} = G - R \quad (2b)$$

where G is the rate of generation and R is the rate of recombination.

$$J_n = D_n \frac{dn}{dx} + \mu_n n d\varphi/dx \quad (3a)$$

$$J_p = D_p \frac{dp}{dx} + \mu_p p d\varphi/dx \quad (3b)$$

where J_n and J_p are the electron and hole current densities.

2.1. Simulation program SCAPS

SCAPS is a software windows application program developed at the University of Gent with Lab window/CVI of national Instruments [16]. The mentioned software has been made available in 1998 to university researchers in the photovoltaic community after the second PV World Conference in Wien [17]. A solar cell simulation problem is stored in an ACSI file, which can be read and completely edited by the graphical user interface of SCAPS [18]. This program is organized on several pages or windows in other jargon languages whereby the user can set parameters and in which results are shown. The user can set an operating point such as temperature, thickness, voltage, frequency, and illumination as well as an action list of calculation to carry out I-V, C-V, C-f, $Q(\lambda)$ [19]. The running parameters in each calculation are (v, f, or λ) varied in the specified range while all other parameters have the value specified in the operating point [20]. Many auxiliary panels can be navigated by the user according to the research material of the study.

As well the user can directly view previously calculated results: I-V, C-V, QE, C-F and also band diagram, electric field carrier densities, partial recombination current. Such results panel is given in Appendix 2, which illustrates the successful result of the previously calculated I-V, C-V, QE, C-F and energy bands after the layers and parameters been added respectively.

3. Methods

The present work includes a numerical simulation of n-TiO₂/p-NiO solar cell using SCAPS-1D to obtain its J-V parameters like V_{oc}, J_{sc}, FF%, efficiency% under AM 1.5 G, 100 mW/cm² standard illumination. The properties varied for the p and n sections were based on past literature and are provided in Table 1 below. The temperature was varied in the range of 300 K to 400 K; the thickness was varied between 2 and 0.05 μ m while the interface state density of 10¹⁸ to 10²¹. The simulations were done without introducing additional defects (Fig. 1).

4. Results and discussions

The variation of current, as a function of wavelength for the p-NiO/n-TiO₂ solar cell, is represented in all the J-V curves presented. Thickness is plotted for each experiment simulation using different parameters relative to different layers. Increased in current as the voltage increased indicated that current in the solar cell depends on voltage and carrier transport mechanism. At high voltages, the high current generated is as a result of high numbers of photo-generated carriers and extended absorption into sub-gap photons.

Table 1

Material properties	n-TiO ₂	p-NiO
Thickness	2.7-0	2-0.05
Bandgap	2.26	3.0
Electron affinity	4.20	3.25
Relative dielectric permittivity	10.00	7.12
CB effective density of states (1/cm ³)	2.0E + 17	2.0E + 17
VB effective density of states (1/cm ³)	6.0E + 17	1.1E + 19
Electron mobility (cm ² /Vs)	1.0E + 2	2.0E + 2
Hole mobility (cm ² /Vs)	25.0	9.0E + 1
Shallow uniform donor density N _D (1/cm ³)	1.0E + 17	0
Shallow uniform acceptor density N _A (1/cm ³)	0	1.0E + 19

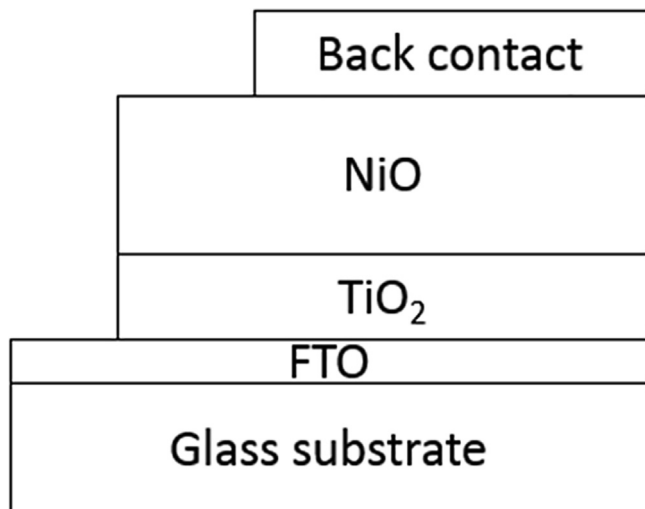


Fig. 1. The set-up of the simulated p-NiO/n-TiO₂ solar cell.

4.1. P-Type thickness variations

Generally, since electron mobility is greater than hole mobility, the p-layer is thicker than n-layer in real-life applications so that an equal number of charge carriers (electrons and holes) could reach the opposite electrodes in almost equal time without getting recombined. The n-layer is usually made smaller so that its width would become less than the diffusion length of holes. Hence, holes in the n-layer can easily diffuse to the metal electrode before recombination occurs. Our simulation covered the variation of the width of both p and n-layer to find the optimum width for the NiO/TiO₂ solar cell system. This optimization further helps to establish why thick absorbers maximize absorption and thin absorbers maximize current collection [21].

For all the thickness varied, the recombination current density remained fairly constant between 1 and 2 mA/cm² while the electrons and holes recombined faster as the thickness reduces. The recombination distances obtained were 3.5 μm, 2.4 μm, 1.9 μm, 1.6 μm, 1.4 μm for corresponding 2, 1, 0.5, 0.1 and 0.05 μm of p-layer thickness varied in this simulation. Therefore, as the thickness of the p-NiO layer reduces, the electrons and holes spend less time to recombine thereby increasing the statistical rate of recombination. Since at higher thickness, the electrons and holes have more time to move before recombining, combined e-h pairs might not lose their energy as heat immediately but can transfer these energies to other existing electrons and holes thereby making the recombination type at high thickness an Auger recombination while those at a lesser thickness of p-layer are non-radiative recombination [22].

The increase in thickness of NiO via the absorber layer gives room for an increase in the number of photons to be absorbed. From Fig. 2, the J_{sc} and efficiency increased as the thickness is varied from 0.05 to 2 except for J_{sc} which decreases from 1 to 2. There was more than 100% increase in Fill Factor (FF) value from 2.5 at 0.05 to 5.21 at 2 μm. The efficiencies are given as 0.03; 0.03; 0.03; 0.04; 0.05 for 0.05; 0.1; 0.5; 1; 2 μm respectively. This means that the efficiency of the solar cell was not dependent on the thickness of less than 1 μm. The increase in J_{sc} and FF and efficiency is as a result of more electron – holes pairs generated as the thickness increase.

4.2. N-type thickness variations

The n-layer which is always the most doped layer creates a wide depletion region located almost entirely in the p-layer. It is important to note that n-layers should be relatively thin compared to p-type to allow the photons to penetrate the layers without getting absorbed much or converted to electron/hole pairs which immediately get separated in the built-in electric field. The recombination profile followed that of the p-layer variation except at the

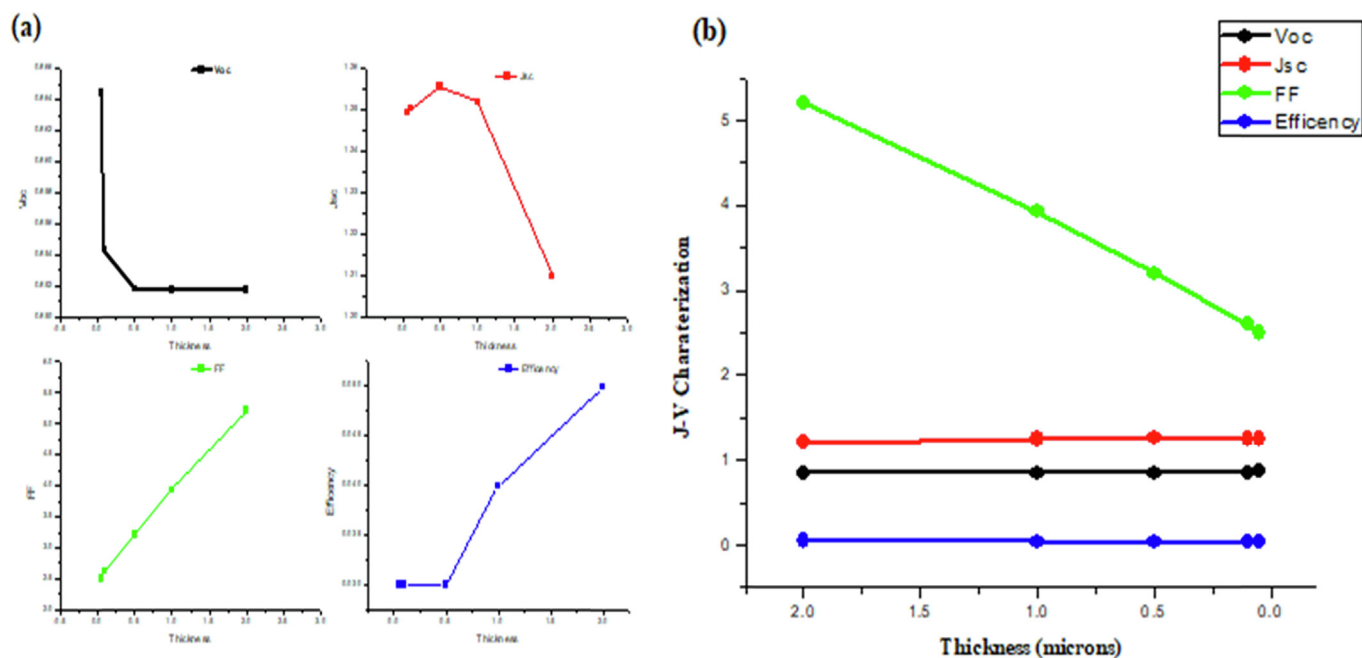


Fig. 2. Plot of (a) V_{oc}, J_{sc}, Fill factor and efficiency (b) J-V characteristics of p-NiO/n-TiO₂ solar cell versus thickness of p-layer in microns.

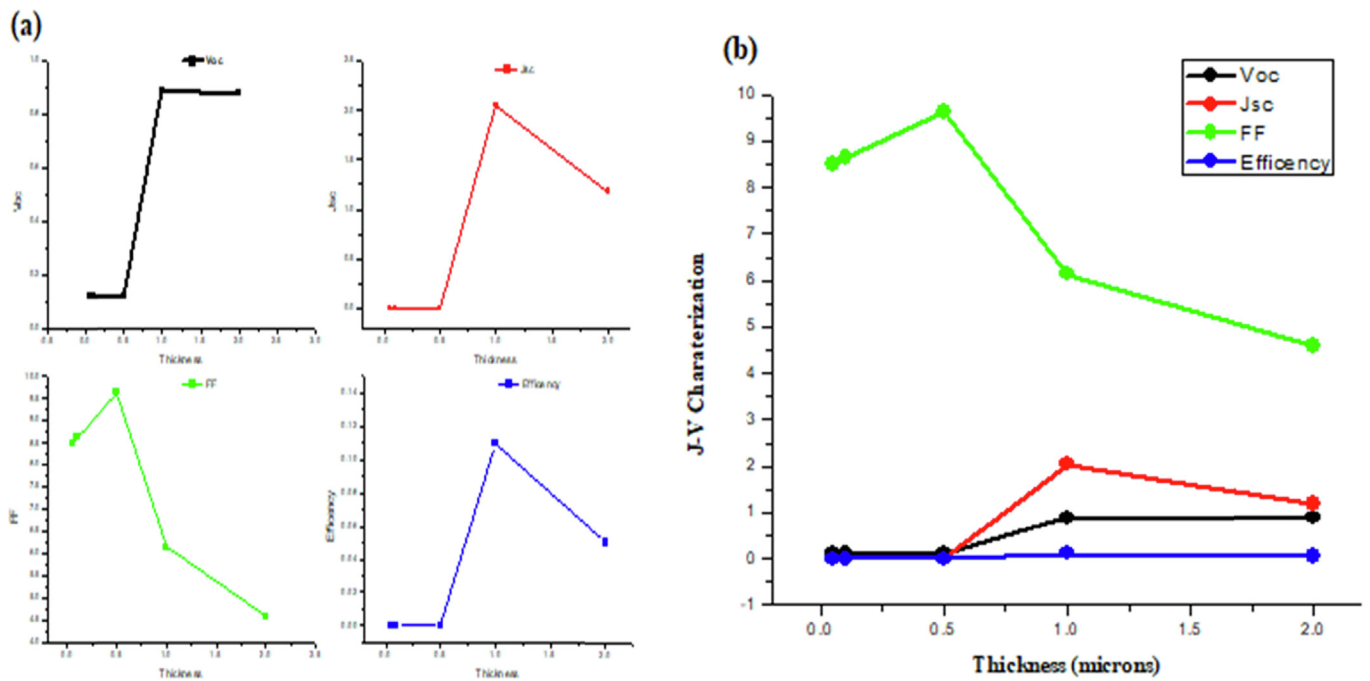


Fig. 3. Plot of (a) V_{oc} , J_{sc} , Fill factor and efficiency (b) J-V characteristics of p-NiO/n-TiO₂ solar cell versus thickness of n-layer in microns.

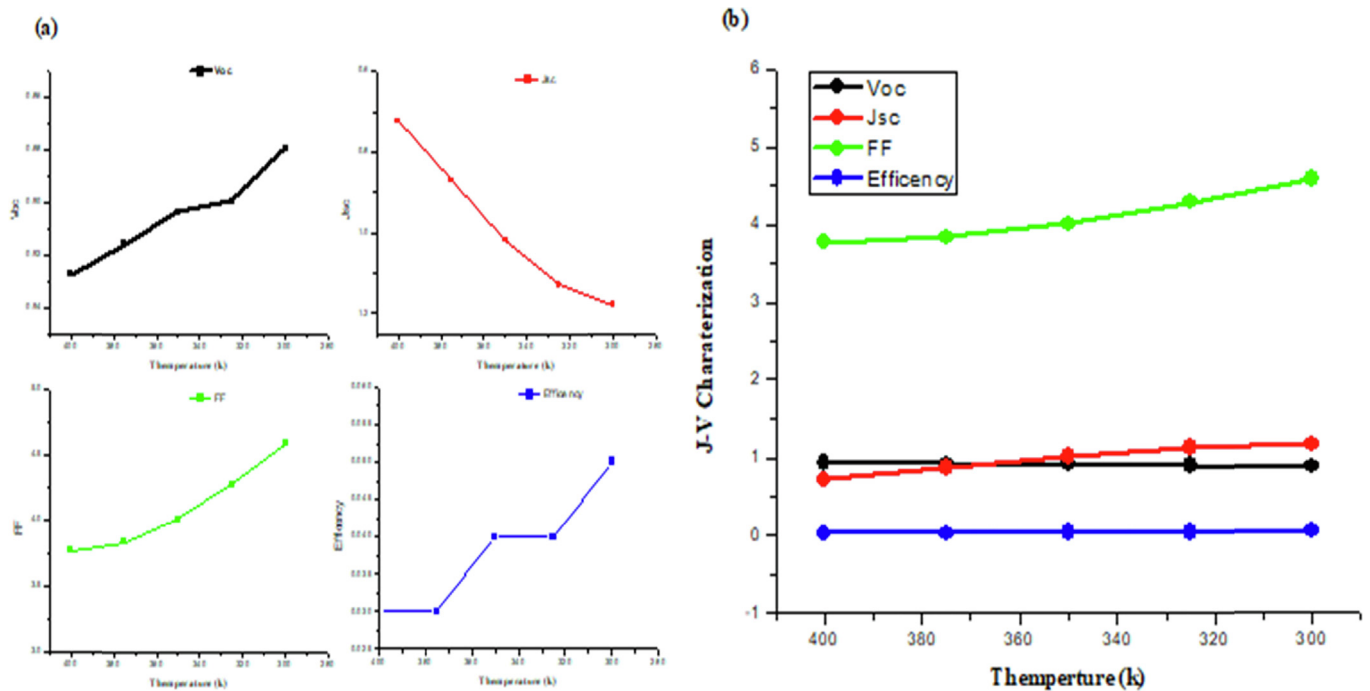


Fig. 4. Plot of (a) V_{oc} , J_{sc} , Fill factor and efficiency (b) J-V characteristics of p-NiO/n-TiO₂ solar cell versus temperature.

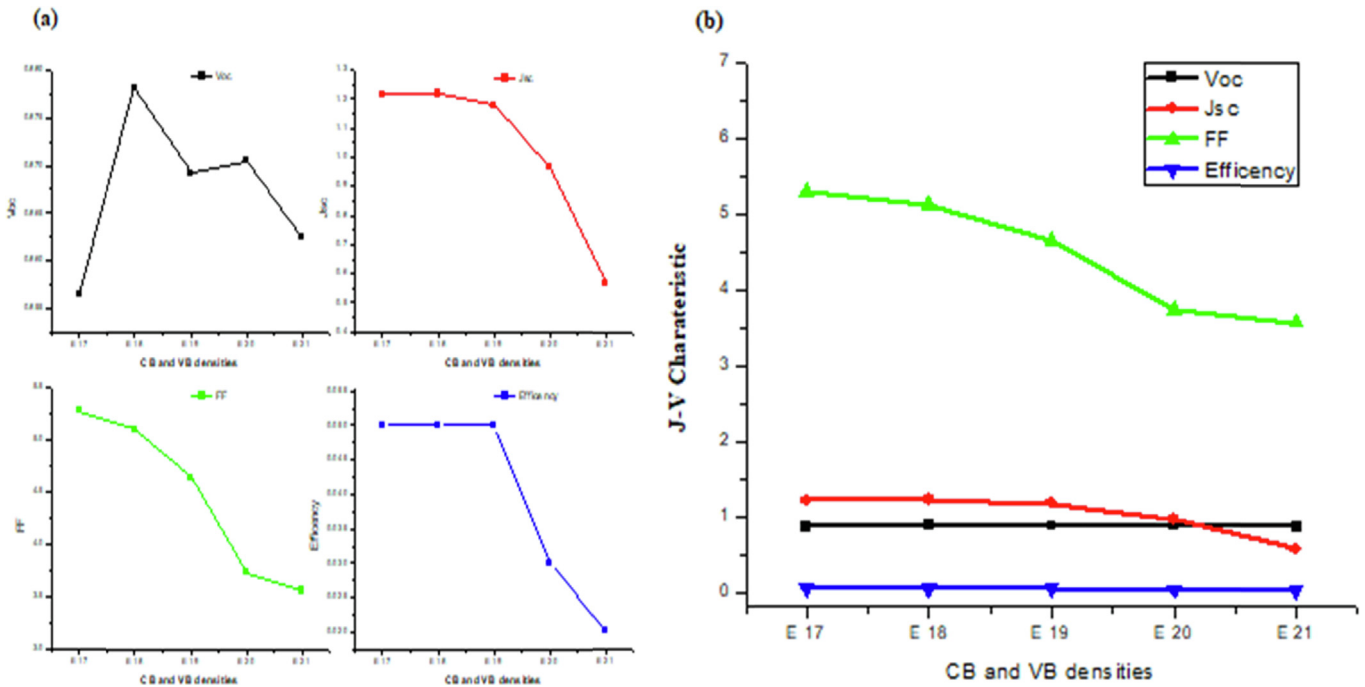


Fig. 5. Plot of (a) V_{oc} , J_{sc} , Fill factor and efficiency (b) J-V characteristics of p-NiO/n-TiO₂ solar cell versus CB and VB density of states for p-layer.

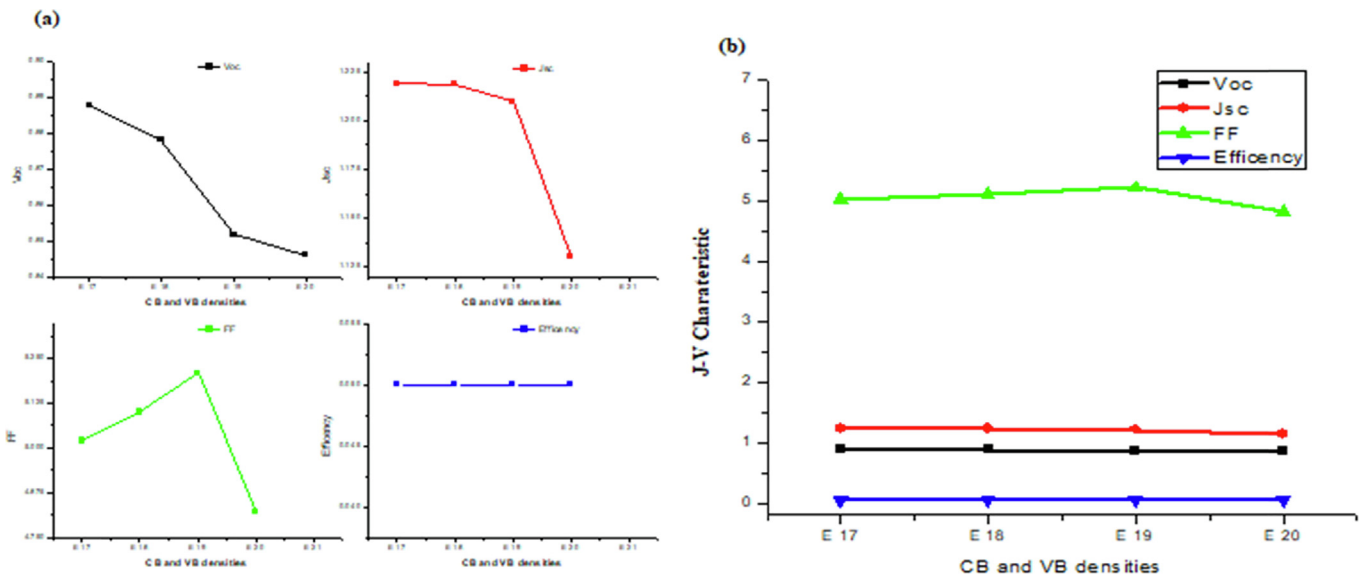


Fig. 6. Plot of (a) V_{oc} , J_{sc} , Fill factor and efficiency (b) J-V characteristics of p-NiO/n-TiO₂ solar cell versus CB and VB density of states for n-layer.

0.5, 0.1 and 0.05 μm thick n-layer. At those thicknesses, the system shows a non-Langevin type of recombination which is not influenced by the layer thickness, yet a good performance is obtained appendix (Appendix 1).

A thicker buffer layer absorbs energy carried by photon resulting in a higher number of photon loss. The SCAP simulation fitted well with the theory as seen in Fig. 3 below. The J_{sc} reduced from 0.05 to 1 μm ; the FF reduced from 0.5 to 2 μm , but this does not have a general implication on the efficiency of the solar cell as shown by the Fig. 3 below. The decrease from 1.5 in 0.01 to 1.1 in 0.5 μm and from 2.05 in 1 to 0.17 in 2 μm is as a result of the fact

that; more thicker buffer layers hastens recombination of holes and is thereby resulting in photon loss and J_{sc} , FF loss.

An increase in temperature reduces the bandgap of a semiconductor and some other parameters. The open-circuit voltage decreases when temperature increases since it depends on I_0 . The short circuit current, J_{sc} , increases slightly with temperature since the bandgap energy E_g decreases and more photons have enough energy to create e-h pairs. However, this is a small effect and the temperature dependence of the short-circuit current by 0.0006 per $^\circ\text{C}$. The recombination distance was fairly constant through-out all temperature variations within the range of

3.5 μ m. Generally, the J-V characteristics (J_{sc} , V_{oc} , FF and $n\%$) are temperature-dependent. J_{sc} , FF and $n\%$ increase with temperature due to reduction in the bandgap energy V_{oc} decrease because it depends directly on the saturation current which in turn decreases within the increase in temperatures. The J_{sc} of (0.72552, 0.871, 1.0166, 1.12829, and 1.17839); FF of (3.77, 3.84, 4.01, 4.28, and 4.59) and n of (0.03, 0.03, 0.04, 0.04, and 0.05) were obtained for 300, 325, 350, 375, and 400 respectively. The V_{oc} obtained was 0.9275, 0.9158, 0.9037, 0.8995, 0.8793 v for the same order of temperature variations as shown in Fig. 4 below.

A higher density of localized states reduces the separation of the quasi-Fermi level and results in lower V_{oc} values. The effect of the carrier mobility in relation to the V_{oc} value is less direct since in open-circuit conditions there is now direct current extraction. The carrier mobility can have an influence in the recombination mechanism, which in open-circuit and steady recombination must equal the generation rate. The V_{oc} drops because of a higher density of states along with J_{sc} and FF values owing to the decreased carrier mobility [23]. The optimal value of efficiency depends on the CB & VB density of states (Fig. 5). The higher values of J_{sc} , FF and $n\%$ were obtained at E18. The J_{sc} and FF decreased fairly on the density of states increase. The density of states does not have a significant effect on the efficiency of the solar cells.

The J_{sc} and FF decreased as the CB and VB density of states increases in the n-type TiO_2 . A decreasing trend of 1.2187, 1.201, 1.209, and 1.130 was observed in J_{sc} for E17, E18, E19, E20, E21. All efficiency remained as 0.05 with an increase in CB and VB density of states of n-type TiO_2 . The V_{oc} also increases with a decrease in the CB and VB density of states from 0.846 to 0.8878v for E20 and E 17 (Fig. 6).

5. Conclusion

The above-mentioned example illustrates the numerical simulation program SCAPS is a valuable tool in film solar cells based

on NiO/ TiO_2 p-n types. This paper was able to give mathematical equation and theoretical optimization of a spin coating NiO/ TiO_2 heterojunction solar cell at 300 to 400 K, 2 to 0.05 μ m and 2 E-17 to 2 E-21 density as the NiO/ TiO_2 thin film structured were studied, this solar cell was optimized for different parameters like the thickness of the p-n absorber layer, the temperature and the density that had a strong impact on the efficiency. All J_{sc} , C-V, FF parameters have been calculated and it was found that the optimized value of the cell thickness varied from 2 to 0.05 for the p-NiO layer and 0 to 2.7 for the n- TiO_2 layer. These results and findings enhance the need to improve and optimized accessibility and sustainable energy that could support further research in thin-film solar cells in affordable and low-income countries.

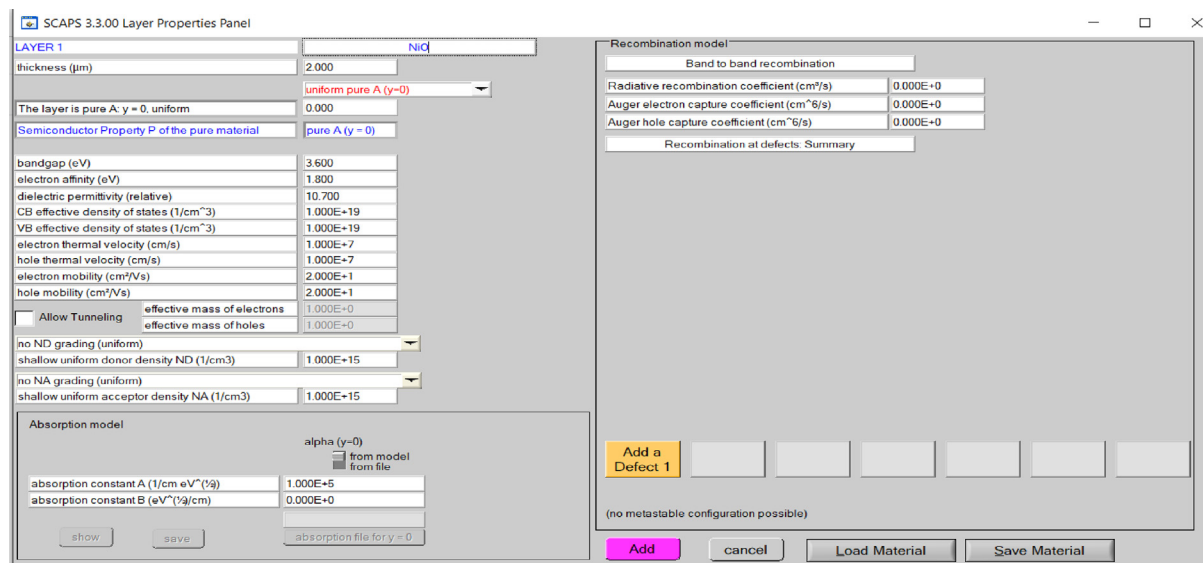
Declaration of Competing Interest

The authors declare that they have no known competing financial interests or personal relationships that could have appeared to influence the work reported in this paper.

Acknowledgments

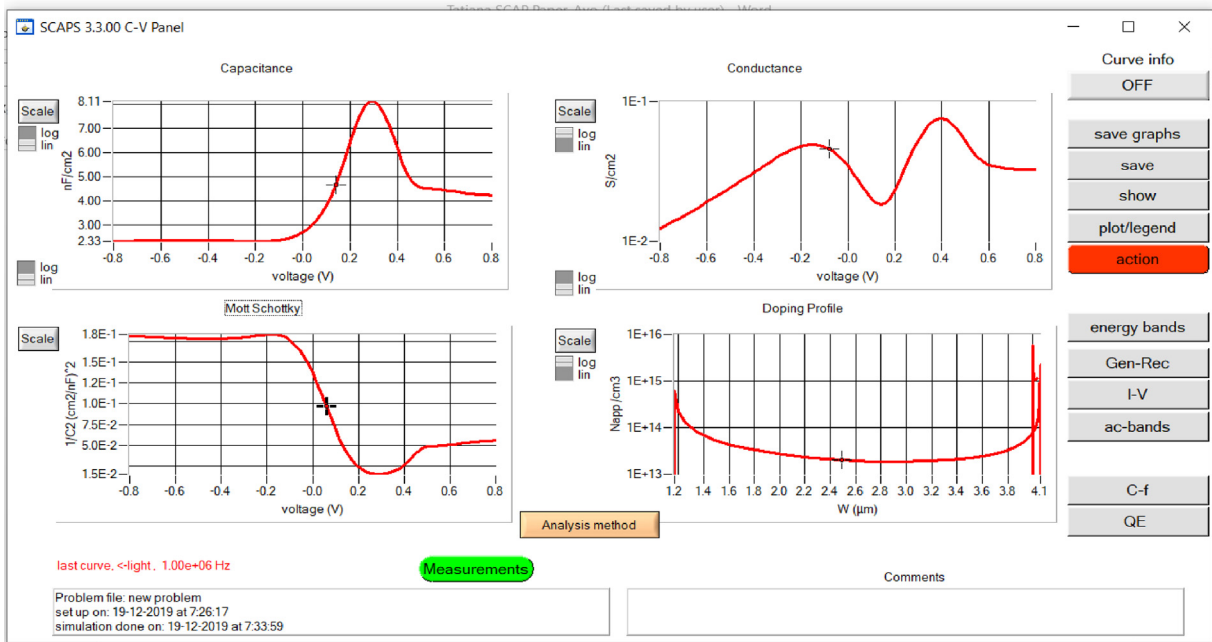
The authors would like to acknowledge and thank the principal author of this SCAPS Software for providing such a veritable tool (simulator program) used in this study. Gratitude goes to the University of Johannesburg South Africa for financial support. Appreciation is also extended to the SCAPS team for allowing the usage of the program. In Acknowledgement, the authors thank the financial support from URC and would also like to thank NRF for financial support.

A



Appendix 1. Typical data input properties panel of the SCAPS graphical user interface allowing to set the parameters of one particular defect level in one particular layer.

B



Appendix 2: An example of a SCAPS panel displaying calculated results: energy band panel, I-V, and QE.

References

- [1] E. Kabir, P. Kumar, S. Kumar, A.A. Adelodun, K.-H. Kim, Solar Energy: Potential and Future Prospects, *Renewable Sustainable Energy Rev.* 82 (2018) 870–905.
- [2] B. Goodenough John, Energy storage materials: a perspective, *Energy Storage Mater.* 1 (2015) 158–161.
- [3] O. Ukoba, F. Inambao, A. Eloka-Eboka, Influence of annealing on properties of spray deposited nickel oxide films for solar cells, *Energy Procedia* 142 (2017) 243–255.
- [4] F. Austin Distributed Disruptions in the Energy Sector. 2017 (Apr 14, 2018). Available: <https://www.brinknews.com/distributed-disruptions-in-the-energy-sector>.
- [5] J. Basden, A. Witkowski, T. Wright, The new make vs buy Calculus how utilities can remain relevant to customers who produce their own power, *Oliver Wyman Energy J.* 2 (2016) 19–21.
- [6] Wikipedia Contributors. Solar Energy. In: Wikipedia, The Free Encyclopedia. 2018. Available from: https://en.wikipedia.org/w/index.php?title=Solar_energy&oldid=84165-4454 [Accessed: May 26, 2018].
- [7] M. Grätzel Photoelectrochemical cells. *Nature.* 2001; 414:338 (11/15/online).
- [8] W.S. Ebhota, P.Y. Tabakov, Hydropower potentials and effects of poor manufacturing infrastructure on small hydropower development in sub-Saharan Africa, *Int. J. Energy Econ. Policy.* 7 (2017) 60–67.
- [9] P. Chelvanathan, M.I. Hossain, N.R. Hamzah, J. Husna, M. Zaman, N. Amin, 21st International Photovoltaic Science and Engineering Conference, November 28th–December 2nd, 2011, Fukuoka, Japan.
- [10] O.K. Ukoba, F. Inambao, A. Eloka-Eboka, 2018, Fabrication of Affordable and Sustainable Solar Cells Using NiO/TiO₂ P-N Heterojunction, *Int. J. Photoenergy* (2018), Hindawi.
- [11] Y.S. Mohammed, M.W. Mustafa, N. Bashir, Hybrid renewable energy systems for off-grid electric power: Review of substantial issues, *Renewable Sustain. Energy Rev.* 35 (2014) 527–539.
- [12] A. Niemegeers, M. Burgelman, *Proc. 25nd IEEE Photovoltaic Spec.Conf., Washington DC, IEEE, New York, 2010, pp. 901–904.*
- [13] A. Niemegeers, S. Gillis, M. Burgelman, 2nd World Conf. Photovoltaic Energy Conv., Wien, ÖE sterreich, July 2010.
- [14] N. Dhar, P. Chelvanathan, M. Zaman, K. Sopian, N. Amin, PV Asia Pacific Conference, 2012, Singapore (published in Elsevier Publication's Energy Procedia 33, 186 (2013)).
- [15] L. Atourki, H. Kirou, A. Ihlal, K. Bouabid, Numerical study of thin films CIGS bilayer solar cells using SCAPS, *Mater. Today.* Proc. 3 (7) (2016) 2570–2577.
- [16] N. Khoshirat, Nurul Amziah Md Yunus, Numerical Simulation of CIGS Thin Film Solar Cells Using SCAPS-1D, 2013 IEEE Conference on Sustainable Utilization and Development in Engineering and Technology.
- [17] H. Movla, Optimization of the CIGS based thin film solar cells: Numerical simulation and analysis, *Optik* (2014) 67–70.
- [18] Y. Nawfal, Jamil, Suha N. Abdulla, Abid A.K. Muhammed, Design and Fabrication Heterojunction Solar cell of Si-CdS-ZnO Thin Film, Proceedings of the international conference nanomaterials: applications and properties, 2012.
- [19] J. Lindahl, U. Zimmermann, P. Szaniawski, T. Törndahl, A. Hultqvist, P. Salomé, C. Platzer-Björkman, M. Edoff, Inline Cu(In, Ga)Se₂ Co-evaporation for high efficiency solar cells and modules, *IEEE J. Photovolt.* (2013) 1100–1105.
- [20] M. Powalla, P. Jackson, W. Witte, D. Hariskos, S. Paetel, C. Tschamber, W. Wischmann, High-efficiency Cu(In, Ga)Se₂ cells and modules *Solar Energy Mater. Solar Cells* (2013) 51–58.
- [21] M. Cl-Steiner, T. Glatzel, M. Rusu, S. Sadewasser, Surface photovoltage analysis of thin CdS layers on polycrystalline chalcopyrite absorber layers by Kelvin probe force microscopy, *Nanotechnology* 19 (14) (2013) 145705.
- [22] S.A. Miller, F.L. Wu, S.L. Ou, R.H. Horng, Kao YC. Improvement in the separation rate of epitaxial lift-off by hydrophilic solvent for GaAs solar cell applications, *Sol. Energy Mater. Sol. Cells* 1 (122) (2014) 233–240.
- [23] Y.R. Galindo-Luna, J. Ibarra-Bahena, R.J. Romero, L. Velazquez-Avelar, C.V. Valdez-Morales, Evaluation of the thermodynamic effectiveness of a plate heat exchanger integrated into an experimental single-stage heat transformer operating with Water/Carrol mixture, *Exp. Therm Fluid Sci.* 51 (2013) 257–263.